Mem. Natl Inst. Polar Res., Spec. Issue, **59**, 168–184, 2006

Scientific paper

The study of the mercury cycle in polar regions: An international study in Ny-Ålesund, Svalbard

Christophe Ferrari[1,2], Pierre-Alexis Gauchard[1], Olivier Magand[1], Katrine Aspmo[3,4], Christian Temme[5], Alexandra Steffen[6], Torunn Berg[3], Johan Ström[7], Aurélien Dommergue[1,5,6], Enno Bahlmann[5], Frédéric Planchon[8], Ralf Ebinghaus[5], Cathy Banic[6], Sonia Nagorski[1], Patrick Baussand[9], Pierre Amato[10,11], Xavier Fain[1], Raphaelle Hennebelle[1], Anne-Marie Delort[11], Martine Sancelme[11], Warren Cairns[12], Carlo Barbante[8,12], Paolo Cescon[8,12], Lars Kaleschke[13] and Claude Boutron[1,14]

[1]*Laboratoire de Glaciologie et Géophysique de l'Environnement du C.N.R.S., 54 rue Molière, BP 96, 38402 Saint Martin d'Hères, France*
[2]*Polytech' Grenoble, Université Joseph Fourier (Institut Universitaire de France), 28 Avenue Benoît Frachon, BP 53, 38041 Grenoble, France*
[3]*Norwegian Institute for Air Research (NILU), Instituttveien 18, P.O. Box 100, N-2027, Kjeller, Norway*
[4]*Department of Chemistry, University of Oslo, P.O. Box 1033, Oslo, Norway*
[5]*Institute for Coastal Research, GKSS Research Centre Geesthacht, D-21502 Geesthacht, Germany*
[6]*Air Quality Research Branch, Meteorological Service of Canada, Environment Canada, 4905 Dufferin St., M3H 5T4-Toronto, Canada*
[7]*Institute of Applied Environmental Research (ITM), Frescativägen 54, S-106 91 Stockholm, Sweden*
[8]*Environmental Sciences Department, University of Venice, Calle Larga S. Marta, 2137, I-30123 Venice, Italy*
[9]*Groupe de Recherche sur l'Environnement et la Chimie Atmosphérique, 39-41 Boulevard Gambetta, 38000 Grenoble, France*
[10]*Laboratoire de Météorologie Physique du CNRS, Université Blaise Pascal (Clermont-Ferrand II), Aubière, France*
[11]*Laboratoire de Synthèse Et Etudes de Systèmes à Intérêts Biologiques (SEESIB), Université Blaise Pascal (Clermont-Ferrand II), Aubière, France*
[12]*Istituto per la Dinamica dei Processi Ambientali del CNR, Dorsoduro, 2137, 30123, Venice, Italy*
[13]*Institute of Environmental Physics, University of Bremen, Germany*
[14]*Unités de Formation et de Recherche de Mécanique et de Physique, Université Joseph Fourier (Institut Universitaire de France), BP 68, 38041 Grenoble, France*
**Corresponding author. E-mail: ferrari@lgge.obs.ujf-grenoble.fr*

(Received April 4, 2005; Accepted January 26, 2006)

Abstract: Mercury (Hg) is a toxic pollutant and it can be strongly accumulated in the food chain, especially in Polar Regions. This paper presents a part of the work that has been on-going for 3–4 years in Ny-Ålesund, Svalbard within the frame of an international collaboration. In Ny-Ålesund in spring 2003, the atmospheric chemistry of mercury has been studied so as to better understand the formation of oxidized mercury species in the atmosphere that could be deposited onto snow surfaces. The role of snow as a potential source of mercury to the atmosphere or as a sink has also been approached to better understand the behavior of this metal. Chemical and biological processes seem to play a major role in Hg storage in snow. When melting, snow could be a major source of Hg into the various ecosystems and this toxin could

therefore be accumulated into the food chain.

key words: mercury, Arctic, deposition, snow, exchanges, accumulation

1. Introduction

Mercury is present in the different reservoirs of the environment in various chemical forms. In the atmosphere, Gaseous Elemental Mercury (GEM, Hg° with concentration ~1.5 ng/m^3) has a lifetime of about one year (Slemr *et al*., 1985). Oxidized species of mercury are found as Particulate Mercury (PM) and Reactive Gaseous Mercury (RGM) at pg/m^3 concentrations. These oxidized species are more reactive and soluble than Hg° and are deposited faster onto environmental surfaces (Lindberg and Stratton, 1998). If Hg° is predominant in the atmosphere, Hg(II) species predominate in aquatic reservoirs (*i.e*. oceans, lakes, cloud water) where it can be transformed into methylmercury by biological processes. This organic form is the most hazardous specie of this metal and can magnify up the food chain in Arctic environments, especially in fish and sea mammals. These ecosystems, including native human populations, are then exposed to this toxic pollutant (Wheatley and Paradis, 1995; Girard and Dumont, 1995).

The reactivity of Hg° in the atmosphere is weak except under special conditions in which Hg° can be rapidly oxidized. These fast atmospheric oxidation processes called Atmospheric Mercury Depletion Events (AMDEs) have been observed in different places in the Arctic and sub-Arctic regions (Schroeder *et al*., 1998; Lindberg *et al*., 2001; Poissant *et al*., 2002; Berg *et al*., 2003; Skov *et al*., 2004), and in Antarctica (Ebinghaus *et al*., 2002; Temme *et al*., 2003). Oxidized Hg species formed by these atmospheric processes (PM and RGM) can be deposited onto the snow surface (Lu *et al*., 2001; Lindberg *et al*., 2002; Berg *et al*., 2003). These AMDEs can be the result of local chemistry and/or the result of transport of air masses already depleted in Hg (Gauchard *et al*., 2005a).

Mercury (Hg) in the snow pack is mainly found dissolved in the snow grains (~94–97% as Hg^{2+} and ~5% as $MeHg^{+}$), while less than 1% is in the interstitial air of snow as Hg° (Ferrari *et al*., 2004a). In Arctic snow packs, Hg° concentrations decrease exponentially with depth (Dommergue *et al*., 2002; Ferrari *et al*., 2004a) probably due to fast oxidation processes of Hg° on the snow crystal surface instead of adsorption of Hg° which seems to be unlikely (Bartels-Rausch *et al*., 2002; Ferrari *et al*., 2004a). The snow pack can then act as a sink for Hg with an incorporation flux estimated to be ~5.8–7.0 pg/m^2/h (Ferrari *et al*., 2004a). In some particular conditions, the snow pack can act as a source of Hg to the atmosphere as a possible result of photo-reduction and photo-initiated reduction of Hg(II) complexes (Dommergue *et al*., 2003a, b).

The increase of mercury deposition flux as recorded in sediments (Lockhart *et al*., 1998) during the last decades may indicate that Hg is accumulated in water systems, where it may become available for methylation. Hg contained in the snow can then enter aquatic ecosystems during snowmelt bridging the atmosphere with aquatic ecosystems.

In this paper, we present a part of the results obtained during the 2003 spring

campaign organised at Ny-Ålesund (Svalbard) to better understand: (1) the chemistry of Hg in the atmosphere and the formation of oxidized species, (2) the fate of mercury inside a sunlight-irradiated snow pack (chemical and bacteria driven mechanisms). This work has been done in the frame of an important network of collaborations as revealed by the number of co-authors of this paper.

2. Material and methods

2.1. Field measurements

2.1.1. Study site

This research program has been conducted in Ny-Ålesund, Svalbard (78°54′N, 11°53′E). Ny-Ålesund is an international scientific village located on the western coast of Spitsbergen, Svalbard (Fig. 1). The study sites were located at two different places in Ny-Ålesund and the results presented here were obtained at the Norwegian research station on the nearby Zeppelin mountain (474 m a.s.l.) and at 300 m far from first Ny-Ålesund habitations, in a cabin (8 m a.s.l.) thereafter called Ny FID-Sund (FID for France Italia Deutschland) at about 100 m from the sea. Snow pit experiments for bacteria collection were also conducted on the Kongsvegen Glacier (see Fig. 1). The

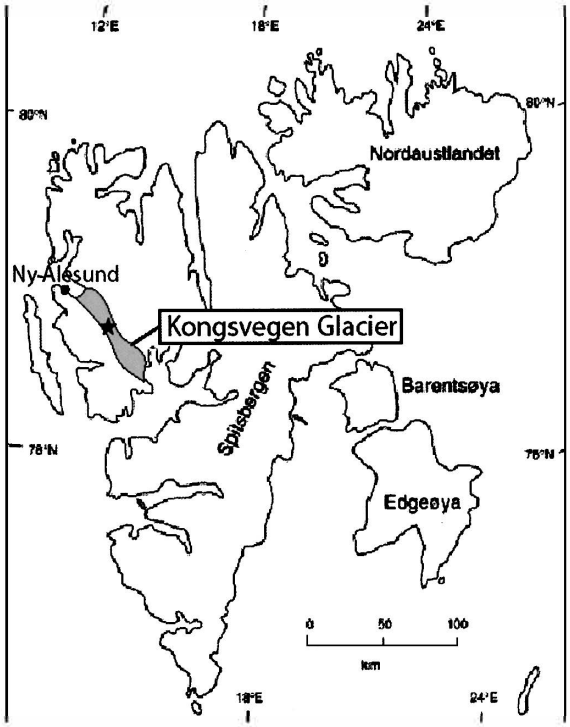

Fig. 1. Localisation of Svalbard, Norway. The field campaign took place both in Ny-Ålesund, North-East of the major island (black spot) and on Kongsvegen Glacier (black star).

front of this glacier is located 10 km southeast from Ny-Ålesund, Svalbard. The sampling area (78°48′N–12°59′E) was chosen in the accumulation area at 600 m altitude, 40 km far from Ny-Ålesund.

2.1.2. Hg° and its speciation in the atmosphere

Gaseous Elemental Mercury (GEM) concentrations were measured using a Tekran 2537A analyzer located in the Ny FID-Sund cabin. The sample air stream is passed alternatively through two gold cartridges where mercury is preconcentrated. Hg is then thermally released and detected by Cold Vapor Atomic Fluorescence Spectrophotometry (CVAFS). The reliability and performance of the Tekran 2537A have been presented in detail elsewhere (Temme *et al*., 2004; Aspmo *et al*., 2005). This instrument was operated with 5 min sampling intervals at a flow rate of 0.8 L/min.

The methods for RGM measurement have been described in detail by Landis *et al*. (2002). RGM was collected on KCl coated annular denuder tubes followed by thermal reduction of RGM and quantification as Hg° with a Tekran 2537A analyzer. For Particulate Mercury (PM) collection and analysis, air was drawn through a quartz particle filter, followed by thermal decomposition of the PM with quantification as Hg° (see Aspmo *et al*., 2005 for details).

2.1.3. Hg° in the snow air

GEM concentrations in the interstitial air of snow were determined at a depth between 10 and 20 cm below the surface (the exact depth depended on sublimation, melting and fresh snow fall and snow drift) using the GAMAS device (Dommergue *et al*., 2002). This GAMAS system, which has been tested successfully in other Arctic sites (see Dommergue *et al*., 2002, 2003a,b and Ferrari *et al*., 2004a for more details), was connected with a cleaned 5 m Teflon line to the Tekran 2537A which was also used for ambient air measurements.

2.1.4. Snow to air flux for Hg°

Hg° emission fluxes from the snow pack to the atmosphere were measured every 5 min using the chamber technique. The flux chamber (FC) was made from a 1 L Nalgene Teflon-FEP bottle, which was cut in half lengthwise. The FC had a volume of 0.5 L and a bottom surface area of ~0.014 m^2. The inlet air was taken from a height of 80 cm above the snow surface in the same height. The analyzer operated with a flushing flow rate of 0.8 L/min. Fluxes were calculated using the following equation:

$$F = (C_a - C_i) \times \left(Q/A \right), \quad (1)$$

with F the flux in ng/m^2/h, C_a the Hg° outlet concentration in ng/m^3, C_i the Hg° inlet concentration in ng/m^3, Q the flushing flow rate in m^3/h and A the bottom surface area in m^2.

2.1.5. Ozone

O_3 was monitored at Ny FID-Sund with an O_3 41M (Environnement S.A, France) analyzer. This technique is based on UV spectrophotometry at 254 nm, with O_3 concentration following the Beer-Lambert law. Method detection limits are ~0.6 ppb, with a precision of 1 ppb. The instrument was setup to output 5 min-averaged data.

2.1.6. Particles

As particles seem to play a role during concomitant Hg and ozone atmospheric

depletion events they were monitored using an optical particle counter (OPC/MPC 301 X/501X analyzer (Malvern, USA)). This instrument measures the quantity of light scattered by individual particles as they pass through a laser beam. Particles with optical diameter between 0.3 and 0.5 μm, 0.5 and 1.0 μm, and 1.0 and 5.0 μm were measured. For more details about these techniques, see Gauchard *et al*. (2005a). At Zeppelin, a Differential Mobility Particle Sizer (DMPS) was used. This instrument measures the electrical mobility of particles. Particles with diameter between roughly 0.02 and 0.70 μm were monitored, and divided into 16 size classes.

2.1.7. Snow collection for Hg

Snow samples (pit and surface) were collected for Hg analysis using ultra-clean procedures described in details by Ferrari *et al*. (2000). Surface snow samples corresponded to the first 1–3 cm of depth and snow pit samples have been collected at three depths (10, 20, and 30 cm) on the 23rd of April 2003 in Ny-Ålesund.

2.1.8. Snow collection for bacteria

Snow samples were collected in two pits dug on the Kongsvegen Glacier (78°48′N–12°59′E, 600 m a.s.l., see Fig. 1) and in Ny-Ålesund by pushing sterile tubes horizontally into the snow at various depths (0–2 m and 0–70 cm respectively). The external layer that maybe air-contaminated, was scratched away using an alcohol sterilized spoon. To avoid any contamination during sampling, sterile gloves and a mask were used.

2.2. Laboratory analysis

2.2.1. Hg in snow

The snow samples were measured for Hg using an Inductively Coupled Plasma Sector Field Mass Spectrometer (ICP-SFMS) as described by Planchon *et al*. (2004). The detection limit was about ~0.2 ng/L. Briefly, each sample was introduced into the instrument inside a class 100 laminar flow clean bench, and was transferred via a Teflon capillary tube into a perfluoroalkoxyl (PFA) microflow nebuliser, where the sample was nebulised into an acid cleaned double-pass PFA spray chamber, and finally was carried into the plasma torch for atomisation and determination. Blank levels were obtained using the same Teflon tubes used for snow collection but filled with pure water when back in the lab from the field. The Teflon tubes for blank determination were transported in the same conditions from field to lab as the Teflon tubes that contained snow. The blanks were found to be close to ~1–2 ng/L.

2.2.2. Bacteria determination

To establish total microbial density profiles, samples were melted and fixed with formaldehyde, and stored at 4°C. 20 m*l* of each fixed sample was stained with a fluorescent dye (DAPI) and the total number of cells was counted by observation with an epifluorescence microscope.

To identify aerobic cultivable micro-organisms, snow samples were kept frozen until the laboratory experiments. Then 0.1 m*l* of melted snow was sampled with cold tips and plated on rich (TS) or poor (R2A) solid media and incubated at three different temperatures (4°C, 15°C, and 28°C). Alternatively liquid TS and R2A media were added to the snow sample, and incubated at 17°C until visible growth (verified by OD_{580nm}, about 1 month of cultivation), and 0.1 m*l* was plated on the corresponding solid

agar media. Taxonomic identifications based on the 16S DNA sequence of each isolated strain were then carried out.

2.3. *Other available parameters*

Meteorological data were available at Zeppelin and in Ny FID-Sund. Backward trajectories at different altitudes were available and have been calculated on the basis of meteorological data from ECMWF (European Centre for Medium-Range Weather Forecasts). Finally, daily GOME-BrO (GOME for Global Ozone Monitoring Experiment) maps were provided by the Institute of Environmental Physics in Bremen (http://www.iup.physik.uni-bremen.de/gomenrt) and were generated using DOAS algorithm on operational GOME level-1 data as described in Richter *et al*. (1998). Potential Frost Flowers coverage area (so called P.F.F.) were obtained as explained by Kaleschke *et al*. (2004).

3. Results and discussion

3.1. *Atmospheric spring chemistry for Hg*

Figures 2a–b show time series of (a) GEM and (b) O_3 measured at Ny FID-Sund (~8 m a.s.l.) from April 15th to May 5th, 2003. During this one-month field experiment, five AMDEs (called AMDEs 1, 2a, 2b, 3 and 4) were recorded.

During AMDE1, low PM and RGM concentrations were recorded, below the detection limit (Fig. 3). Event 2a occurred with high PM concentrations (~100–200 pg/m^3)(Fig. 3). Also higher RGM concentrations were recorded (~30–50 pg/m^3) (Fig. 3). PM and RGM were even higher during AMDE2b (~200 pg/m^3) (Fig. 3).

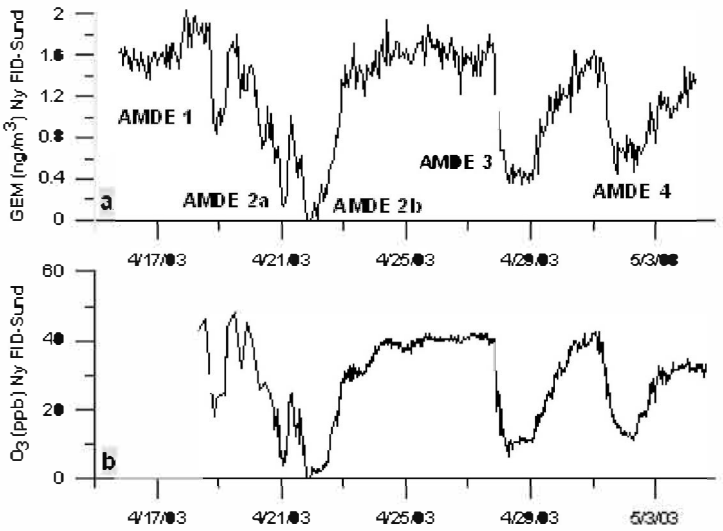

Fig. 2. Time series of (a) GEM and (b) O_3 measured at Ny FID-Sund from April 15th to May 5th. The five recorded AMDEs (1, 2a, 2b, 3 and 4) are shown.

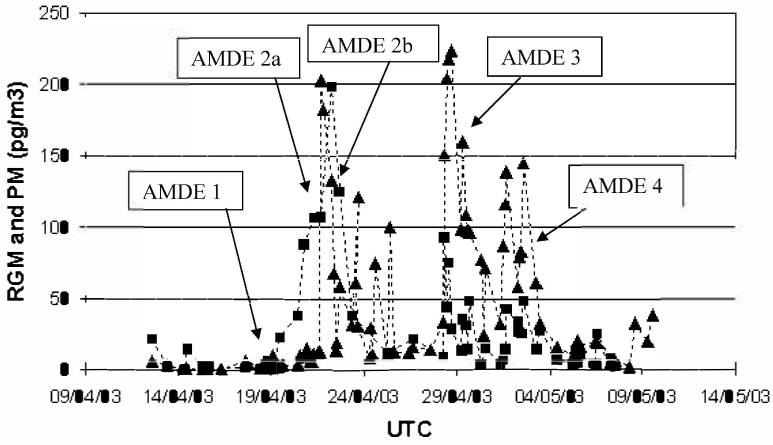

Fig. 3. Time series of RGM (triangles) and PM (squares) measured at Zeppelin Station from April 15th to May 5th.

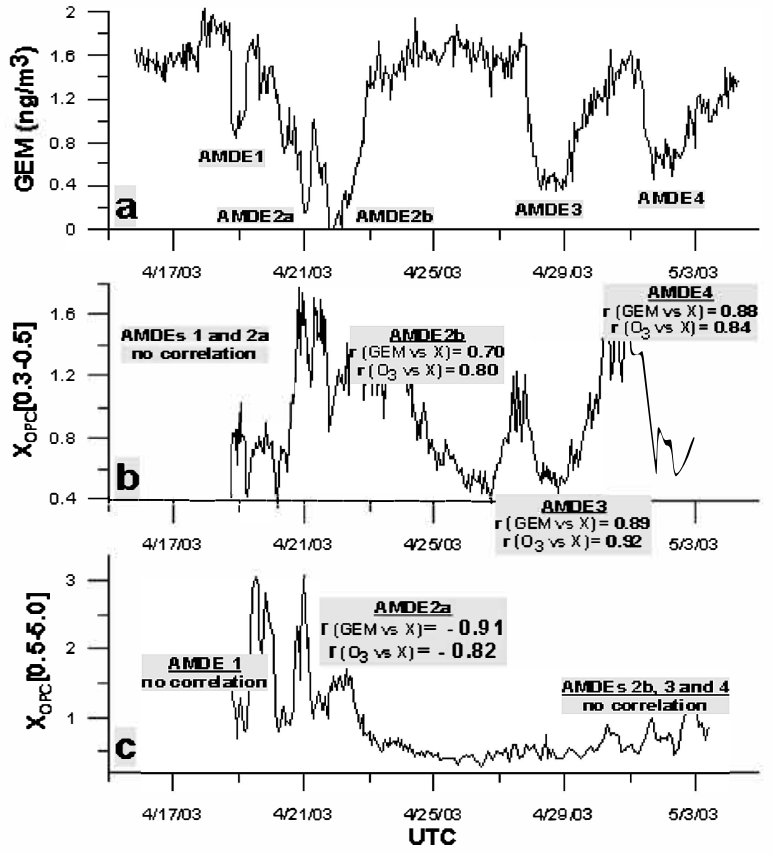

Fig. 4. Time series from April 15th to May 5th of (a) GEM at Ny FID-Sund, and variations of (b) smaller OPC particles and (c) larger OPC particles during AMDEs. When correlations were observed, linear correlation coefficients (for particles vs GEM or O_3) are also given.

Finally, AMDEs 3 and 4 showed similar characteristics for RGM with relatively high concentrations (~200 pg/m^3), and lower PM concentrations (~50 pg/m^3) (Fig. 3). Because the particle counters were not directly comparable (the two systems do not use the same physical properties of atmospheric particles for quantification) and as we were interested only in particle variations during AMDEs and LOEs, the particles were hereafter expressed as a relative parameter (Figs. 4 and 5). This parameter was calculated (for all size classes shared by both instruments) as the ratio between the concentration of particles and the mean value of particles during the entire sampling period. Two ratios were defined for particles measured with the OPC: X_{OPC} [0.3–0.5] for "smaller particles" *i.e.* within the 0.3–0.5 μm range and X_{OPC} [0.5–5.0] for "larger particles" *i.e.* in the range from 0.5 to 5.0 μm (Fig. 4). Two ratio were also defined for DMPS measurements: X_{DMPS} [0.02–0.4] and X_{DMPS} [0.56–0.71], for particles with diameters between 0.02 and 0.4 μm and between 0.56 and 0.71 μm, respectively (Fig. 5). Some positive and negative correlations can be found directly on the figure between

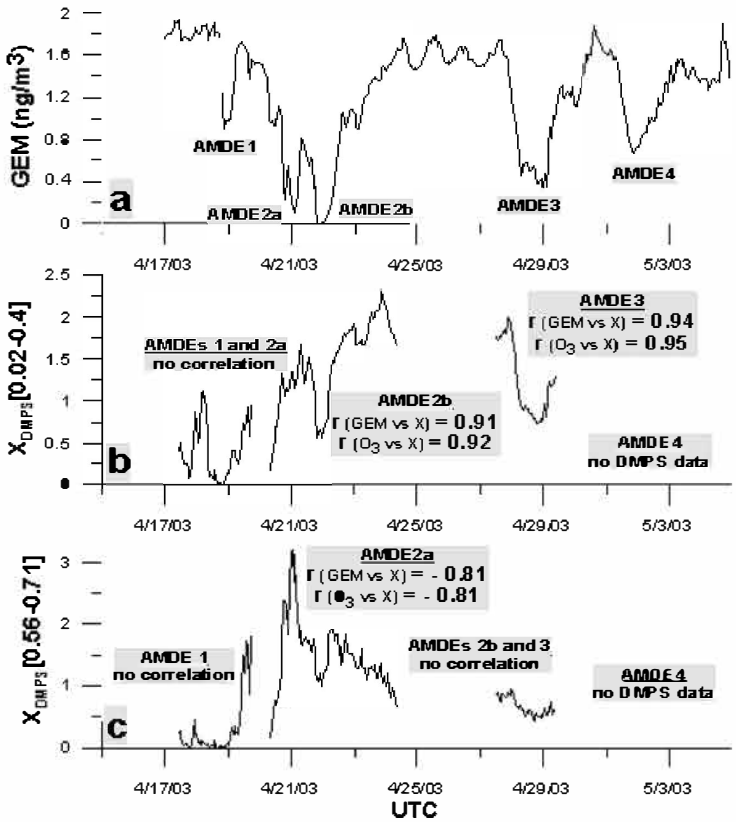

Fig. 5. Time series from April 15th to May 5th of (a) GEM at Zeppelin, and variations of (b) smaller DMPS particles and (c) larger DMPS particles during AMDEs. When correlations were observed, linear correlation coefficients (for particles vs GEM or O_3) are also given.

GEM and particles, according to their size (Figs. 4 and 5). When it had a meaning, linear correlation coefficients were calculated (for particles vs GEM and O_3, *cf*. Figs. 4 and 5). *P*-values were found to be less than 0.0001 for each correlation.

In order to try to understand if these AMDEs were from local or non-local origin, O_3 apparent destruction rates ($\Delta O_3/\Delta t$) were calculated during AMDEs and compared to theoretical rates obtained with a combined BrO-ClO mechanism for ozone destruction (see Tuckermann *et al*., 1997). For these authors, apparent destruction rates of ~4.5 ppb/h or more can only be attributed to advection of air masses already depleted in O_3. The use of meteorological data can give us indications about the transport of the air masses. Nevertheless, data such as wind in Ny-Ålesund have to be taken with caution due to the fact that local wind direction is strongly influenced by topography and wind speeds may sometimes be influenced locally as well, due to catabatic winds and the ridges making up Svalbard. In addition, when focusing on AMDEs transport aspect, GOME-BrO observations were combined with calculated backtrajectories (see Sommar *et al*., 2004 for details). GOME maps must be taken with great care since these maps represent the whole tropospheric column.

Finally, RGM to PM respective concentrations were discussed. If the distribution of mercury during a depletion event is higher in PM relative to RGM this may indicate that the depletion occurred elsewhere and the already depleted air masses were transported to the measurement site. Conversely, if the distribution of mercury species is higher in RGM than PM, then it can be an indication of a more local event (Lindberg *et al*., 2002).

To conclude, the use of all these parameters (*e.g*. O_3 apparent destruction rates and GEM, O_3 and particle relative decrease or increase rates, meteorological data, GOME-BrO maps and backtrajectories and RGM/PM ratios) have to be taken individually with care but all together they can provide useful indications of the possible origins of the AMDEs.

Events 1 and 2a present characteristics of events due to advection of already depleted air masses as RGM and PM concentrations were low, indicating that these oxidized Hg species have probably been deposited during the air mass transport. During AMDE2a, an increase of large (diameters in the range 0.5–1.0 μm) atmospheric particle concentrations was observed, similar to previous recordings of a transport event in the sub-Arctic (Gauchard *et al*., 2005b). Furthermore, the apparent destruction rate of O_3 (~(−5) to (−6) ppb/h) was high for both AMDE1 and AMDE2a indicating that this event was more the result of already depleted air masses. GOME-BrO maps and back trajectories (see Gauchard *et al*., 2005a) did not show high levels of BrO, neither at the monitoring area, nor at places over which the air masses passed in the last 6 days. Furthermore, higher PM and RGM concentrations than for AMDE1 were observed during this event, but with higher PM relative to RGM than during events 2b, 3 and 4. Thus, event 2a is the result of advection of an already depleted air mass.

PM and RGM were higher during AMDE2b, with higher RGM relative to PM than during event 2a. Lower apparent O_3 destruction rates (~2.2 ppb/h) were measured for this event. All these facts support the conclusion that AMDE2b was a more local event. Concerning GOME-BrO maps and back trajectories, low levels of BrO were observed in the Svalbard area but at the beginning of this AMDE, air masses

arriving in Ny-Ålesund traveled through high BrO level areas. We see here another difference between AMDE2b and the two former events. AMDE2b seems to be characterized by more local chemistry, which can be a mix between chemistry and non-long range transport (<500 km).

RGM concentrations increased in comparison to PM during event 3. Event 4 shows similar characteristics to event 3, where the RGM was relatively high, and PM was low. O_3 apparent destruction rates stayed low (~3 ppb/h). High levels of BrO were observed for both events in the area of Svalbard with GOME-BrO maps. Furthermore, the origin of air masses ending in our study area during these events shows that these often passed over areas with elevated BrO concentrations. These results indicate that these events could be more local events and/or a non-long range transport.

The most common assumption to explain O_3 destruction and GEM oxidation is the production of radical Br via the photolysis of compounds like Br_2 or BrCl. Reactions involving gas phase reservoirs, as originally proposed, are not sufficient to account for the bromine observed (Barrie *et al*., 1988). A number of heterogeneous reactions have therefore been put forward, and the source of molecular bromine active compounds is believed to be the oxidation of Br- in aerosols, snow and frozen surfaces (Foster *et al*., 2001).

Frost flowers are ice crystals which grow on newly-formed sea ice from a saturated water vapor layer. They provide a large effective surface area and a reservoir of sea-salt ions with assumed consequent implications for LOEs and AMDEs (Rankin *et al*., 2002). Frost flowers growth depends (1) on the existence of new ice which is formed in leads (linear breaks in the sea ice cover) or polynyas (openings between drift ice and fast ice or the coast) and (2) of a strong negative temperature gradient above the ice surface (*e.g*. strong negative air temperature, $\sim -20^{\circ}C$) (Kaleschke *et al*., 2004). During event 2b, Potential Frost Flowers (P.F.F.) area was evaluated (see Kaleschke *et al*., 2004 for details) and presented in Fig. 6. For event 2b (Fig. 6) frost flowers seemed to have been formed north and East of Svalbard. During that event, wind came from north east. The air mass measured in Ny-Ålesund could then have been enriched in active bromine originating from frost flowers emission, leading to a regional depletion of Hg and ozone, as observed in event 2b. The simulation of P.F.F. for event 3 and 4 does not show clear evidence of frost flower formation around Svalbard.

3.2. Deposition of Hg onto snow surfaces

Contrary to what has been observed in different Arctic sites during AMDEs (Lu *et al*., 2001; Lindberg *et al*., 2002; Berg *et al*., 2003), mercury concentrations in surface snow do not fluctuate greatly during the period of study from April to May 2003 (Fig. 7). When comparing Hg concentrations in snow sampled during AMDE periods and non-AMDE periods, we can observe no real difference. For the two first AMDEs (1 and 2a), the fact that no Hg deposition onto snow surfaces was observed (Fig. 3) could be explained as these two AMDEs had a long range transport origin, corresponding more to air masses already depleted in Hg. The AMDE 2b (Fig. 2) could be attributed to a more local chemistry but no significant increase in Hg concentration in surface snow had been observed after the event. Events 3 and 4 are likely to have a regional (*i.e*.

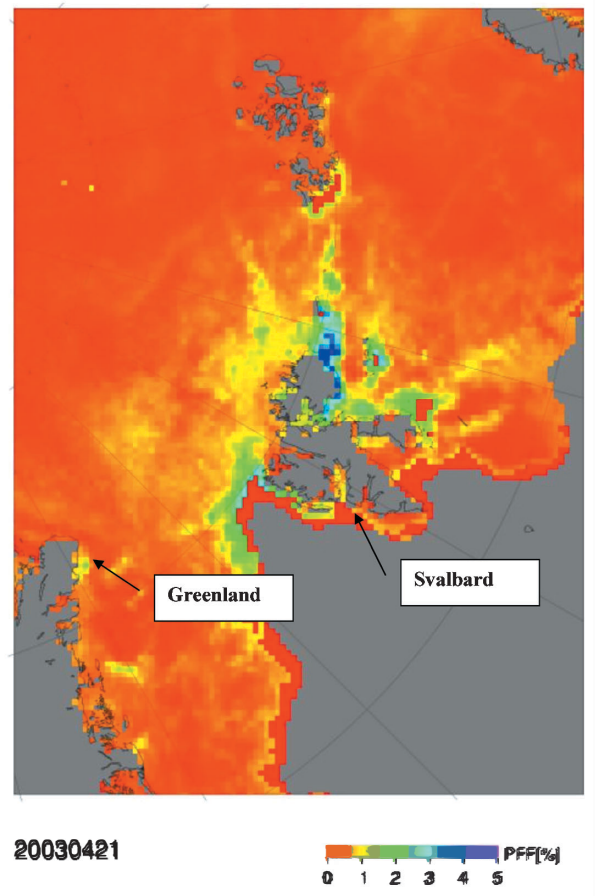

Fig. 6. Potential Frost Flower (P.F.F.) coverage area obtained for event 2b following the method described by Kaleschke et al. (2004).

~10^2 km, see Gauchard *et al.*, 2005a) origin. The fact that no Hg concentration change in surface snow was observed for both AMDEs 3 and 4 could be explained by a really heterogeneous Hg deposition over regional surfaces for these kinds of events. This observation could have, if confirmed, an important environmental consequence since high deposition fluxes could be then spatially restricted.

3.3. Role of snow on the Hg budget

The Hg concentrations measured in the snow layers of a pit dug on April 23rd, 2003, were ~8 ng/L and the concentrations reported for Hg° in interstitial air of snow ranged from ~0.8–25 ng/m^3. Hg in the seasonal snow pack of Ny-Ålesund consisted mainly of Hg(II) (more than 99%), while Hg° in the snow air represented less than 1%. This Hg balance is in general agreement with the balance obtained by Ferrari *et al.* (2004a) for the Greenland snow pack.

In most cases, Hg° concentrations in the snow air (~0.8–25 ng/m^3) were higher

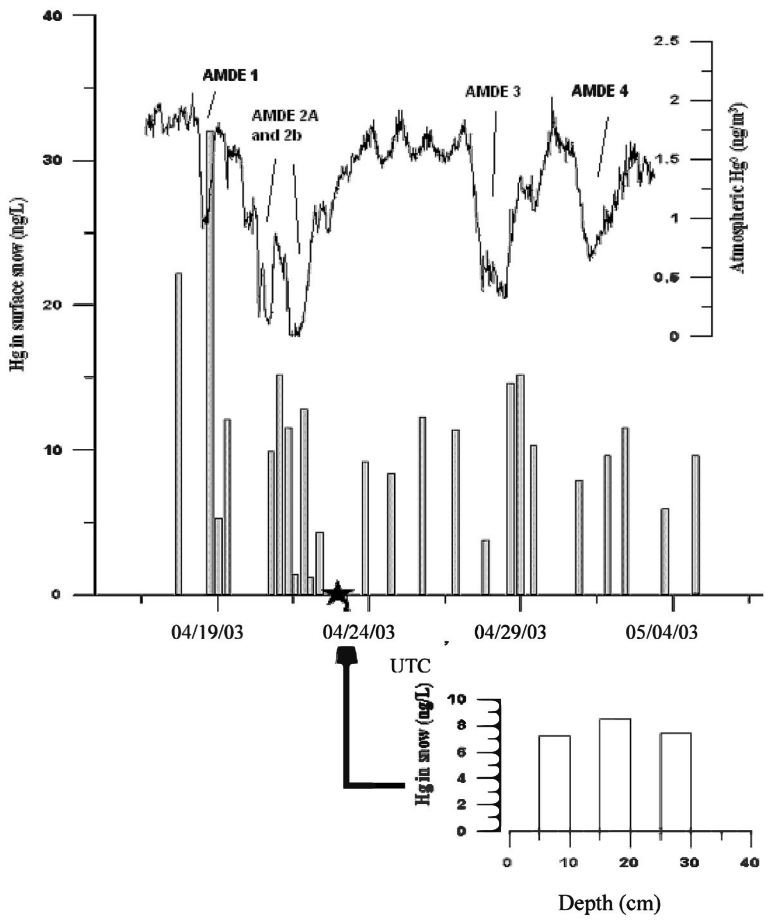

Fig. 7. Hg in surface snow (ng/L) (gray vertical bars) and Ambient Hg° (ng/m³) (black line) for April 16th to May 4th, 2003 at Ny-Ålesund,. For April 23, 2003, the Hg concentration in a pit dug near the Ny FID-Sund cabin was measured from the surface to the bottom of the snow pack (vertical open bars).

than Hg° in the atmosphere above the snow pack (~1.5–1.6 ng/m^3) (Fig. 8a-b). This was always true during the first time period (April 15th to April 21st, see Fig. 8a and b) and usually true during the second time period (April 22nd to May 3rd; see Fig. 8a and b). In some cases, the concentration of Hg° in the snow air was lower (*e.g.* 0.8–1.1 ng/m^3) than the atmospheric concentrations (*e.g.* 1.5–1.6 ng/m^3) leading to an incorporation of Hg° in the snow pack except during AMDEs. This phenomenon has already been observed elsewhere (Dommergue *et al.*, 2003a; Ferrari *et al.*, 2004a, b) shortly after polar sunrise. The calculated incorporation flux of Hg° in the snow air (see Ferrari *et al.* (2004a) for calculation details) in this study was ~5–40 pg/m^2/h, which is only slightly higher than what has been previously calculated by Ferrari *et al.* (2004a) as ~5.8–7.0 pg/m^2/h.

If the periods of incorporation were short in time, the periods of production were

clearly dominating the profiles. The emission flux from the snow pack to the atmosphere, neglecting the ventilation by wind is evaluated (see Dommergue *et al*. (2003b) for details) as ~(0.3–6.5) ng/m^2/h, which is in agreement with the production fluxes measured or calculated for other Arctic and sub-Arctic sites, *i.e*. ~1.5–2.5 ng/m^2/h (Dommergue *et al*., 2003b), and ~1–8 ng/m^2/h (Schroeder *et al*., 2003).

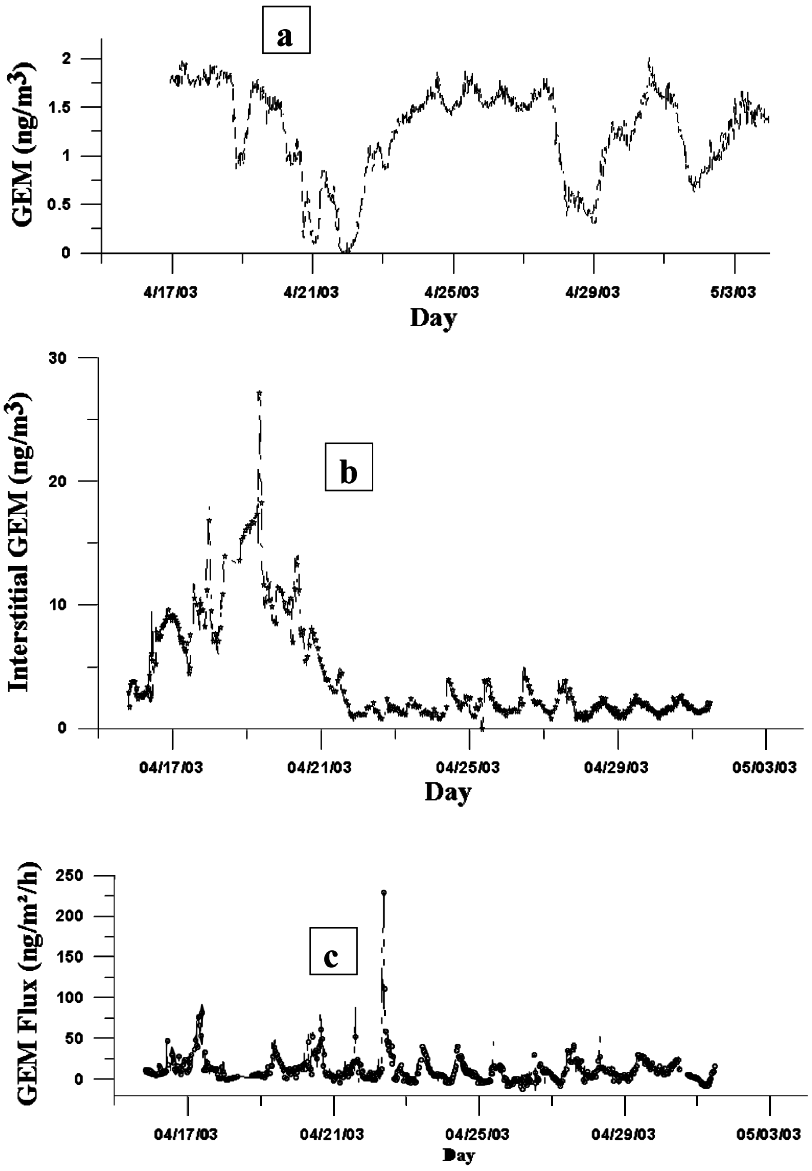

Fig. 8. (a) Ambient GEM concentrations (ng/m^3), (b) snow-pack interstitial air Hg$^\circ$ concentrations at 10–20 cm below the surface (ng/m^3), (c) Hg$^\circ$ flux from the snow to the atmosphere (ng/m^2/h), for April 16th to May 4th, 2003 at Ny-Ålesund,.

It seems that the production process should be largely enhanced when snow temperature is increasing, as the result of increasing the surface of quasi-liquid layers on the snow grains, leading to a higher emission flux of Hg° from the snow to the atmosphere. The production of Hg° was not driven only by temperature but was also linked to irradiation (Dommergue *et al*., 2003a; Ferrari *et al*., 2004a). This suggests a photochemical mechanism, as described by both field and laboratory experiments (Lalonde *et al*., 2002; Dommergue, 2003). Contrary to what was observed for the Hg° concentration in interstitial air (Fig. 8b), the Hg° measured flux profile (Fig. 8c) did not exhibit two different patterns during the period of study. The Hg° flux from the snow pack to the atmosphere exhibited a diurnal pattern correlated with solar irradiation for the whole period of study. The emission flux of Hg° to the atmosphere seems to be governed by atmospheric parameters (especially irradiation) but not by snow parameters (temperature,…).

3.4. Impact of biological processes on the Hg budget: preliminary results

If a chemical process has been highlighted in the snow pack, the role of bacteria on Hg cycle is still under discussion. Firstly, our results show that the global bacterial densities at the two sites were nearly the same, about 10^4 to 10^5/m*l* of melted snow. These values are consistent with data collected under similar environments. However

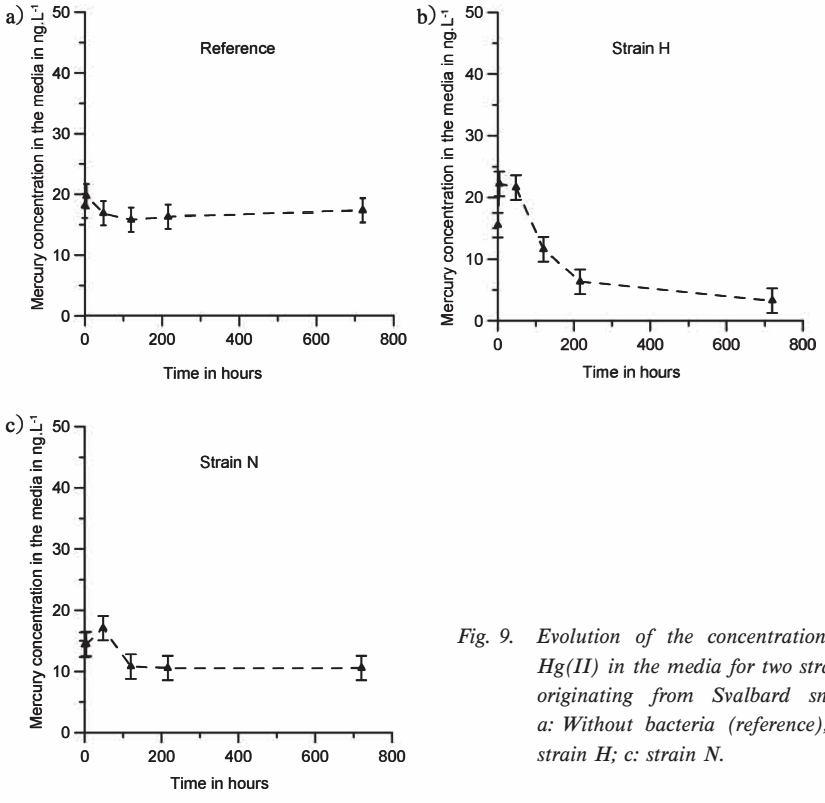

Fig. 9. Evolution of the concentration of Hg(II) in the media for two strains originating from Svalbard snow. a: Without bacteria (reference); b: strain H; c: strain N.

some differences can be observed depending on the sampled layers, particularly the maximal counts were obtained for the deepest layer corresponding to the summer layer. The melting of the summer layer was observed for this glacier and leads to a development of bacteria and then an increase in their number.

Secondly, concerning the cultivable fraction of micro-organisms, we have isolated 12 bacteria, 5 yeasts and 1 fungus. Most of these micro-organisms were pigmented (pigments are well-known to protect cells against cold and UV radiations). They are able to grow at low temperatures and on low nutriment media. Identification of the isolated strains shows three bacterial phyla, (i) Proteobacteria, (ii) Firmicutes and (iii) Actinobacteria. Each bacterium has been exposed to a low level of Hg (~50 ng/L) in R2A solution and the concentration of Hg has been measured over a 30 day experiment. Preliminary results show different trends for Hg exposed to bacteria. This is the case for strain H (Fig. 9b) compared to the solution without bacteria (Fig. 9a). But for strain N, no interaction was observed (Fig. 9c). Understanding the possible mechanisms to explain such trends is in progress.

4. Conclusion

This paper presents the first results obtained in the scientific village Ny-Ålesund in spring 2003 where different groups studied the chemistry of Hg and the role of snow on the accumulation of this metal in ecosystems. Atmospheric processes seem to play a key role on Hg deposition onto the snow surface but complex transformations (chemical and biological) appear to take place in the snow pack itself. Field and laboratory measurements need to be performed so as to understand the reasons of the observed Hg concentration increase in the Arctic food chain.

Acknowledgments

This research was funded by different national institutions, the French polar Institute I.P.E.V. (Institut Paul-Emile Victor, program CHIMERPOL 399), the A.D.E.M.E. (Agence de l'Environnement et de la Maîtrise de l'Energie, Programme 0162020), the French Ministry of Environment and Sustainable Development and the CNRS (Centre National de la Recherche Scientifique). Claude Boutron and Christophe Ferrari thank the Institut Universitaire de France (I.U.F.) for its financial help for this research. We thank Franck Delbart, Martin Mellet from the I.P.E.V. and Jens Kube, John Deary for their constant help during the field experiments. We would like to express our great thanks to the Alfred Wegener Institute (A.W.I.) and especially the Koldewey Station and its staff, the Norwegian Polar Institute and the Kings Bay for their help during our stay. We all thanks Torunn Berg and NILU to have organized this international Hg campaign in this wonderful place.

References

Aspmo, K., Gauchard, P.-A., Steffen, A., Temme, C., Berg, T. and 8 other authors (2005): Measurements of atmospheric mercury species during an international study of mercury depletion events at Ny-

Ålesund, Svalbard, spring 2003. How reproducible are our present methods? Atmos. Environ., **39**, 7607–7619.

Barrie, L.A., Bottenheim, J.W., Schnell, R.C., Crutzen, P.J. and Rasmussen, R.A. (1988): Ozone destruction and photochemical reactions at polar sunrise in the lower Arctic atmosphere. Nature, **334**, 138–141.

Bartels-Rausch, T., Jöri, M. and Ammann, M. (2002): Adsorption of mercury on crystalline ice, Annual Report 2002—Laboratory for radiochemistry and environmental chemistry—. Paul Scherrer Institut, Villigen, Switzerland.

Berg, T., Sekkesaeter, S., Steinnes, E., Valdal, A-K. and Wibetoe, G. (2003): Springtime depletion of mercury in the European Arctic as observed at Svalbard. Sci. Total Environ., **304**, 43–51.

Dommergue, A. (2003): Dynamique du mercure dans les neiges de hautes et moyennes latitudes, Etudes in situ et en conditions simulées des mécanismes de réactivité chimique et d'échanges. PhD thesis, University of Grenoble, 2003 (http: //lgge.obs.ujf-grenoble.fr/publiscience/theses/these-dommergue.pdf).

Dommergue, A., Ferrari, C.P. and Boutron, C.F. (2002): First investigation of an original device dedicated to the determination of gaseous mercury in interstitial air of snow. Anal. Bioanal. Chem., **375**, 106–111.

Dommergue, A., Ferrari, C.P., Poissant, L., Gauchard, P.-A. and Boutron, C.F. (2003a): Chemical and photochemical processes at the origin of the diurnal cycle of gaseous mercury within the snow-pack at Kuujjuarapik, Whamagoostui, Québec. Environ. Sci. Technol., **37**, 3289–3297.

Dommergue, A., Ferrari, C.P., Gauchard, P.-A., Boutron, C.F., Poissant, L., Pilote, M., Jitaru P. and Adams, F. (2003b): The fate of mercury species in a sub-arctic snowpack during snowmelt. Geophys. Res. Lett., **30**, 1621, doi: 10.1029/2003GL017308.

Ebinghaus, R., Kock, H., Temme, C., Einax, J., Löwe, A., Richter, A., Burrows, J. and Schroeder, W.H. (2002): Antarctic springtime depletion of atmospheric mercury. Environ. Sci. Technol., **36**, 1238–1244.

Ferrari, C.P., Moreau, A.L. and Boutron, C.F. (2000): Clean conditions for the determination of ultra-low levels of mercury in ice and snow samples. Fresenius J. Anal. Chem., **366**, 433–437.

Ferrari, C.P., Dommergue, A. and Boutron, CF. (2004a): Profiles of mercury in the snow pack at Station Nord, Greenland shortly after polar sunrise. Geophys. Res. Lett., 31, L03401, doi: 10.1029/2003GL 018961.

Ferrari, C.P., Dommergue, A., Boutron, C.F., Skov, H. and Jensen, B. (2004b): Nighttime production of elemental gaseous mercury in interstitial air of snow at Station Nord, Greenland. Atmos. Environ., **38**, 2727–2735.

Foster, K.L., Plastridge, R.A., Bottenheim, J., Shepson, P.B., Finlayson-Pitts, B.J. and Spicer, C.W. (2001): The role of Br2 and BrCl in surface ozone destruction at polar sunrise. Science, **291**, 471–474.

Gauchard, P.-A., Aspmo, K., Temme, C., Steffen, A., Ferrari, C. and 11 other authors (2005a): Characterizing Atmospheric Mercury Depletion Events recorded during an international study of mercury in Ny-Ålesund, Svalbard, spring 2003. Atmos. Environ., **39**, 7620–7632.

Gauchard P.-A., Ferrari, C.P., Dommergue, A., Poissant, L., Pilote, M., Gueheneux, G., Boutron, C.F. and Baussand, P. (2005b): Atmospheric particle evolution during a nighttime atmospheric mercury depletion event in sub-Arctic at Kuujjuarapik/Whapmagoostui, Québec, Canada. Sci. Total Environ., **336**, 215–224.

Girard, M. and Dumont, C. (1995): Exposure of James Bay Cree to methylmercury during pregnancy for the years 1983–91. Water Air Soil Pollut., **80** (1), 13–19.

Kaleschke, L., Richter, A., Burrows, J., Afe, O., Heygster, G., Notholt, J., Rankin, A.M., Roscoe, H.K., Hollwedel, J. and Wagner, T. (2004): Frost flowers on sea ice as a source of sea salt and their influence on tropospheric halogen chemistry. Geophys. Res. Lett., **31**, L16114.

Lalonde, J.D., Poulain, A.J. and Amyot, M. (2002): The role of mercury redox reactions in snow on snow-to-air mercury transfer. Environ. Sci. Technol., **36**, 174–178.

Landis, M.S., Stevens, R., Schaedlich, F. and Prestbo, E. (2002): Development and characterization of an annular denuder methodology for the measurement of divalent inorganic reactive gaseous mercury in ambient air. Environ. Sci. Technol., **36**, 3000–3009.

Lindberg, S.E. and Stratton, W.J. (1998): Atmospheric mercury speciation: concentrations and behaviour of reactive gaseous mercury in ambient air. Environ. Sci. Technol., **32**, 49–57.

Lindberg, S.E., Brooks, S., Lin, C.-J., Scott, K., Meyers, T., Chambers, L., Landis, M. and Stevens, R. (2001):

Formation of reactive gaseous mercury in the Arctic: Evidence of oxidation of Hg to gas-phase Hg-II compounds after Arctic sunrise. Water Air Soil Pollut., **1** (5/6), 295–302.

Lindberg, S.E., Brooks, S., Lin, C.-J., Scott, K.J., Landis , M.S., Stevens, R.K., Goodsite, M. and Richter, A. (2002): Dynamic oxidation of gaseous mercury in the Arctic troposphere at polar sunrise. Environ. Sci. Technol., **36**, 1245–1256.

Lockhart, W.L., Wilkinson, P., Billeck, B.N., Danell, R.A., Hunt, R.V., Brunskill, G.J., Delaronde, J. and St. Louis, V. (1998): Fluxes of mercury to lake sediments in central and northern Canada inferred from dated sediment cores. Biogeochemistry, **40**, 163–173.

Lu, J.Y., Schroeder, W.H., Barrie, L.A., Steffen, A., Welch, H.E., Martin, K., Lockhart, L., Hunt, R.V., Boila, G. and Richter, A. (2001): Magnification of atmospheric mercury deposition to polar regions in springtime: the link to tropospheric ozone depletion chemistry. Geophys. Res. Lett., **28**, 3219–3222.

Planchon, F.A.M., Gabrielli, P., Gauchard, P.-A., Dommergue, A., Barbante, C. and 9 other authors (2004): Direct determination of mercury at sub-picogram per gram level in polar snow and ice by ICP-SFMS. J. Anal. Atomic Spectrosc., **19**, 823–830 doi: 10.1039/B402711F.

Poissant, L., Dommergue, A. and Ferrari, C.P. (2002): Mercury as a global pollutant. J Phys. IV, ed. by C. F. Boutron. EDP Sciences, 143–160.

Rankin, A.M., Wolff, E.W. and Martin, S. (2002): Frost flowers: implications for tropospheric chemistry and ice core interpretation. J. Geophys. Res., **107**, 4683–4697.

Richter, A., Wittrock, F., Eisinger, M. and Burrows, J. (1998): GOME observations of tropospheric BrO in Northern Hemisphere spring and summer 1997. Geophys. Res. Lett., **25**, 2683–2686.

Schroeder, W.H., Anlauf, K.G., Barrie, L.A., Lu, J.Y., Steffen, A., Schneeberger, D.R. and Berg, T. (1998): Arctic springtime depletion of mercury, Nature, **394**, 331–332.

Schroeder, W.H., Steffen, A., Scott, K., Bender, T., Prestbo, E., Ebinghaus, R., Lu, J.Y. and Lindberg, S. (2003): Summary report: first international Arctic atmospheric mercury research workshop Conference Report. Atmos. Environ., **37**, 2551–2555.

Skov, H., Christensen, J., Goodsite, M.E., Heidam, N.Z., Jensen, B., Wåhlin, P., Geernaert, G. (2004): Fate of elemental mercury in the Arctic during atmospheric mercury depletion episodes and the load of atmospheric mercury to the Arctic. Environ. Sci. Technol., **38**, 2373–2382.

Slemr, F., Schuster, G. and Seiler, W. (1985): Distribution, speciation, and budget of atmospheric mercury. J. Atmos. Chem., **3**, 407–434.

Sommar, J., Wängberg, I., Berg, T., Gardfeldt, K., Munthe, J., Richter, A., Urba, A., Wittrock, F. and Schroeder, W. (2004): Circumpolar transport and air-surface exchange of atmospheric mercury at Ny-Ålesund (79°N), Svalbard, spring 2002. Atmos. Chem. Phys. Discuss., **4**, 1727–1771.

Temme, C., Einax, J.W., Ebinghaus, R. and Schroeder, W.H. (2003): Measurements of atmospheric mercury species at a coastal site in the Antarctic and over the South Atlantic Ocean during polar summer. Environ. Sci. Technol., **37**, 22–31.

Temme, C., Aspmo, K., Bahlmann, E., Banic, C., Berg, T. and 9 other authors (2004): Repeatability and reproducibility of data from different groups and locations in Ny-Ålesund during the hg-campaign 2003. RMZ-Mater. Geoenviron., **51**, 2042–2045.

Tuckermann, M., Ackermann, R., Gölz, C., Lorenzen-Schmidt, H., Senne, T., Stutz, J., Trost, B., Unold, W. and Platt, U. (1997): DOAS-observation of halogen radical-catalysed arctic boundary layer ozone destruction during the ARCTOC-campaigns 1995 and 1996 in Ny-Ålesund, Spitsbergen. Tellus, **49B**, 533–555.

Wheatley, B. and Paradis, S. (1995): Exposure of Canadian aboriginal peoples to methyl mercury. Water Air Soil Pollut., **80**, 3–11.